

# Fifth-order attosecond polarization beats using twin color-locked noisy lights in cascade three-level system with Doppler-free approach

Jianping Song (宋建平)<sup>1</sup>, Yu Feng (冯宇)<sup>1</sup>, Chenli Gan (甘琛利)<sup>1</sup>, Long Li (李隆)<sup>1</sup>,  
Yuanyuan Li (李院院)<sup>1</sup>, Xiaojun Yu (余孝军)<sup>1</sup>, Hao Ge (葛浩)<sup>1</sup>, Ruiqiong Ma (马瑞琼)<sup>1</sup>,  
Chuangshe Li (李创社)<sup>1</sup>, Xiangchen Zhang (张相臣)<sup>1</sup>, Yanpeng Zhang (张彦鹏)<sup>1</sup>, and Keqing Lu (卢克清)<sup>2</sup>

<sup>1</sup>Department of Electronic Science and Technology, Xi'an Jiaotong University, Xi'an 710049

<sup>2</sup>State Key Laboratory of Transient Optics and Technology, Xi'an Institute of Optics and Precision Mechanics, Chinese Academy of Sciences, Xi'an 710068

Received September 8, 2004

Fifth-order attosecond sum-frequency polarization beat (FASPB) is studied in a cascade three level system with the phase-conjugation fourth-order coherence function theory. An improved schematic diagram of geometry, which is different from that inducing fifth-order femtosecond different-frequency polarization beat (FFDPB), is used to obtain FASPB. By analyzing the cases that pump beams have either narrow or broad bandwidth, it is found that the temporal behavior of the sum-frequency polarization beat signal depends on the properties of the lasers and transverse relaxation rate of the atomic energy-level system. Finally, the cascaded four-wave mixing (FWM) processes and the difference between attosecond and femtosecond polarization beats have been discussed, it is found that cascaded or sequential lower processes can often obscure the direct fifth-order polarization beat processes.

OCIS codes: 320.7110, 030.1640, 030.6600, 190.4380.

Nonlinear effects of high order on polarization beats have attracted a lot of attention recently<sup>[1-7]</sup>. Zhang *et al.*<sup>[2-7]</sup> investigated the higher-order stochastic correlation effects of Markovian field in the femtosecond difference-frequency polarization beats (FDPBs).

In this paper, fifth-order attosecond sum-frequency polarization beats (FASPBs) using twin color-locked noisy lights in cascade three-level system are studied.

Fifth-order polarization beat in cascade three-level atomic system is a polarization beat phenomenon originating from the interference between one- and two-photon six-wave-mixing (SWM) processes. Figure 1 shows a cascade three-level atomic system with ground state  $|0\rangle$ , intermediate state  $|1\rangle$ , and excited state  $|2\rangle$ . States between  $|0\rangle$  and  $|1\rangle$  and between  $|1\rangle$  and  $|2\rangle$  are coupled by dipolar transition with resonant frequencies  $\Omega_1$  and  $\Omega_2$ , respectively, while state between  $|0\rangle$  and  $|2\rangle$  is dipolar forbidden. The schematic diagram of the geometry of FASPB (see Fig. 2) shows a double-frequency time-delay four-wave mixing (FWM) and SWM polarization beats, in which beams 1 and 2 consist of two frequency components  $\omega_1$  and  $\omega_2$ , while beam 3 has frequency  $\omega_3$ . All the incident beams are linearly polarized in the same direction. The beat signals (beams 4 and 5) have the same polarization as the incident beams propagate along a direction almost opposite to that of beam 2. The beat signal is detected by a photodiode. We assume that  $\omega_1 \approx \Omega_1$ ,  $\omega_2 \approx \Omega_2$ , and  $\omega_3 \approx \Omega_1$ , therefore  $\omega_1$  and  $\omega_2$  will drive the transitions from  $|0\rangle$  to  $|1\rangle$  and from  $|1\rangle$  to  $|2\rangle$ , respectively. Beam 4 represents the signal of FWM caused by the third-order polarization beats, and beam 5 represents the signal of SWM caused by the fifth-order polarization beats. In fifth-order polarization beats<sup>[7]</sup>, one-photon degenerate SWM signals with frequency  $\omega_3$  will be emitted along the direction  $\mathbf{k}_3 + 2\mathbf{k}_1 - 2\mathbf{k}'_1$ , and

two-photon non-degenerate SWM signals with frequency  $\omega_3$  will be emitted along the directions  $\mathbf{k}_3 + 2\mathbf{k}_2 - 2\mathbf{k}'_2$  and  $\mathbf{k}_3 + \mathbf{k}_1 - \mathbf{k}'_1 + \mathbf{k}_2 - \mathbf{k}'_2$ . In the phase-conjugation geometry, beams 4 and 5 have a small angle between them.

In a typical experiment, the two-color light sources enter a dispersion-compensated Michelson interferometer to generate identical twin composite beams. Twin composite stochastic fields of beam 1,  $E_{p1}(\mathbf{r}, t)$  and beam 2,  $E_{p2}(\mathbf{r}, t)$  can be written as

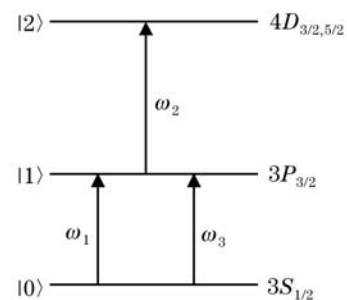


Fig. 1. Cascade three-level configuration.

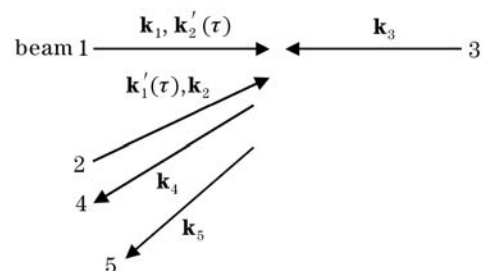


Fig. 2. Schematic diagram of the geometry of FASPB.

$$\begin{aligned}
 E_{p1} &= A_1(\mathbf{r}, t) \exp(-i\omega_1 t) + A_2'(\mathbf{r}, t) \exp(-i\omega_2 t) \\
 &= \varepsilon_1 u_1(t) \exp[i(\mathbf{k}_1 \cdot \mathbf{r} - \omega_1 t)] \\
 &\quad + \varepsilon_2' u_2(t - \tau) \exp[i(\mathbf{k}_2' \cdot \mathbf{r} - \omega_2 t + \omega_2 \tau)],
 \end{aligned}$$

$$\begin{aligned}
 E_{p2} &= A_1'(\mathbf{r}, t) \exp(-i\omega_1 t) + A_2(\mathbf{r}, t) \exp(-i\omega_2 t) \\
 &= \varepsilon_1' u_1(t - \tau) \exp[i(\mathbf{k}_1' \cdot \mathbf{r} - \omega_1 t + \omega_1 \tau)] \\
 &\quad + \varepsilon_2 u_2(t) \exp[i(\mathbf{k}_2 \cdot \mathbf{r} - \omega_2 t)].
 \end{aligned}$$

where  $\varepsilon_i$ ,  $\mathbf{k}_i$  ( $\varepsilon_i'$ ,  $\mathbf{k}_i'$ ) are the constant field amplitude and the wave vector of  $\omega_i$  frequency component in beam 1 (beam 2), respectively.  $u_i(t)$  is a dimensionless statistical factor that contains phase and amplitude fluctuation [i.e.,  $u_i(t) = a_i(t) \exp[i\theta_i(t)]$ ], here  $a_i(t)$  contains pure amplitude fluctuation, while  $\theta_i(t)$  contains pure phase fluctuation.  $u_i(t)$  is taken to be a complex ergodic stochastic function of  $t$ , which obeys complex circular Gaussian statistics in chaotic field.  $\tau$  is a variable relative time delay between the prompt (unprime) and delayed (prime) fields. To accomplish this, the lights of frequency components  $\omega_1$  and  $\omega_2$  are split and recombined to provide two double-frequency pulses in such a way that  $\omega_1$  frequency component is delayed by  $\tau$  in beam 2 and  $\omega_2$  frequency component is delayed by the same amount in beam 1 (see Fig. 2). The time delay  $\tau$  is introduced in both composite beams, which is quite different from that of FDPBs. On the other hand, beam 3 is assumed to be a quasi-monochromatic light, the complex electric fields of beam 3 can be written as

$$\begin{aligned}
 E_{p3} &= A_3(\mathbf{r}, t) \exp(-i\omega_3 t) \\
 &= \varepsilon_3 u_3(t) \exp[i(\mathbf{k}_3 \cdot \mathbf{r} - \omega_3 t)],
 \end{aligned}$$

where  $\omega_3$ ,  $\varepsilon_3$ , and  $\mathbf{k}_3$  are the frequency, the field amplitude, and the wave vector of beam 3, respectively, and  $u_3(t) \approx 1$  for quasi-monochromatic light.

We employ perturbation theory to calculate the density matrix elements by following perturbation channels.

$$(I) \rho_{00}^{(0)} \xrightarrow{A_1} \rho_{10}^{(1)} \xrightarrow{(A_1')^*} \rho_{00}^{(2)} \xrightarrow{A_1} \rho_{10}^{(3)} \xrightarrow{(A_1')^*} \rho_{00}^{(4)} \xrightarrow{A_3} \rho_{10}^{(5)},$$

$$(II) \rho_{00}^{(0)} \xrightarrow{A_1} \rho_{10}^{(1)} \xrightarrow{(A_1')^*} \rho_{11}^{(2)} \xrightarrow{A_1} \rho_{10}^{(3)} \xrightarrow{(A_1')^*} \rho_{11}^{(4)} \xrightarrow{A_3} \rho_{10}^{(5)},$$

$$(III) \rho_{00}^{(0)} \xrightarrow{A_1} \rho_{10}^{(1)} \xrightarrow{(A_1')^*} \rho_{11}^{(2)} \xrightarrow{A_2'} \rho_{21}^{(3)} \xrightarrow{(A_2)^*} \rho_{11}^{(4)} \xrightarrow{A_3} \rho_{10}^{(5)},$$

$$(IV) \rho_{00}^{(0)} \xrightarrow{A_3} \rho_{10}^{(1)} \xrightarrow{A_2'} \rho_{20}^{(2)} \xrightarrow{(A_2)^*} \rho_{10}^{(3)} \xrightarrow{A_2'} \rho_{20}^{(4)} \xrightarrow{(A_2)^*} \rho_{10}^{(5)},$$

$$(V) \rho_{00}^{(0)} \xrightarrow{A_3} \rho_{10}^{(1)} \xrightarrow{A_2'} \rho_{20}^{(2)} \xrightarrow{(A_1')^*} \rho_{21}^{(3)} \xrightarrow{(A_2)^*} \rho_{11}^{(4)} \xrightarrow{A_1} \rho_{10}^{(5)},$$

$$(VI) \rho_{00}^{(0)} \xrightarrow{A_3} \rho_{10}^{(1)} \xrightarrow{A_2'} \rho_{20}^{(2)} \xrightarrow{(A_1')^*} \rho_{21}^{(3)} \xrightarrow{A_1} \rho_{20}^{(4)} \xrightarrow{(A_2)^*} \rho_{10}^{(5)}.$$

In perturbation chains (I), (II), and (III), we note that the roles of complex amplitudes  $A_1$  and  $(A_1')^*$ ,  $A_2$  and  $(A_2')^*$  can be interchangeable, respectively, and the total perturbation chains of the SWM signals are fifteen. We

are mainly interested in the beat signal with modulation frequency  $\omega_2 + \omega_1$  (i.e., atttosecond sum-frequency polarization beat signal), so there are two beating approaches (I), (II), (III), (V), (VI) and (III), (IV), (V), (VI).

The nonlinear polarization  $P^{(5)}$  responsible for the phase-conjugate SWM signal is given by averaging over the velocity distribution function  $w(\mathbf{v})$ . Thus  $P^{(5)} = N\mu_1 \int_{-\infty}^{+\infty} d\mathbf{v} w(\mathbf{v}) \rho_{10}^{(5)}(\mathbf{v})$ , here  $\mathbf{v}$  is the atomic velocity,  $N$  is the density of atoms. For a Doppler-broadened atomic system (inhomogeneous broadening extremely overwhelms the homogeneous width), we have  $w(v) = \frac{1}{\sqrt{\pi}u} \exp[-(v/u)^2]$ , where  $u = \sqrt{2k_B T/m}$ ,  $m$  is the mass of an atom,  $k_B$  is Boltzmann's constant, and  $T$  is absolute temperature.

For sake of analytical simplicity, the polarization beat signal can be calculated from two different limit approximations, extreme Doppler-broadened limit (i.e.,  $k_3 u \rightarrow \infty$ , inhomogeneous broadening limit) and extreme Doppler-free limit (i.e.,  $k_3 u \rightarrow 0$ ). For simplicity, here we neglect the Doppler effect.

The atomic response to Markovian stochastic optical fields, including chaotic fields, phase-diffusing fields, and real Gaussian fields, etc., are now largely well understood. We assume that the laser source is a chaotic fields which are characterized by the fluctuation of both amplitude and phase of the field. It is used to describe a multi-mode laser source. The random function  $u_i(t)$  of the complex noisy fields is taken to obey complex circular Gaussian statistics when its fourth-order coherence function satisfies<sup>[3,8]</sup>

$$\begin{aligned}
 &< u_i(t_1) u_i(t_2) u_i^*(t_3) u_i^*(t_4) > \\
 &= < u_i(t_1) u_i^*(t_3) > < u_i(t_2) u_i^*(t_4) > \\
 &\quad + < u_i(t_1) u_i^*(t_4) > < u_i(t_2) u_i^*(t_3) > .
 \end{aligned}$$

We assume that laser sources have Lorentzian line shape, then

$$< u_i(t_1) u_i^*(t_2) > = \exp(-\alpha_i |t_1 - t_2|) \quad (i = 1, 2),$$

where  $\alpha_i = \frac{1}{2} \delta\omega_i$  is the auto correlation decay of the noisy light, and  $\delta\omega_i$  is the line width of  $\omega_i$  frequency component.

SWM signal intensity can be well approximated by  $I \propto |< P^{(5)} >|^2$ .

We first consider the case that twin composite beams 1 and 2 are narrow band so that  $\alpha_1 \ll \Gamma_{10}$  and  $\alpha_2 \ll \Gamma_{20}$ . This is the case where the dephasing time is much shorter than the correlation time of the incoherent light. From channels (I), (II), (III), (V), (VI), the fifth-order beat signal intensity is

$$\begin{aligned}
 I(\tau, r) &\propto |B_1|^2 \exp(-4\alpha_1 |\tau|) \\
 &\quad + |\eta B_2|^2 \exp[-2(\alpha_1 + \alpha_2) |\tau|] + \exp[-(3\alpha_1 + \alpha_2) |\tau|] \\
 &\quad \times \{ \eta B_1^* B_2 \exp[-i\Delta k \cdot r + i(\omega_2 + \omega_1)\tau] \\
 &\quad + \eta^* B_1 B_2^* \exp[i\Delta k \cdot r - i(\omega_2 + \omega_1)\tau] \}. \quad (1)
 \end{aligned}$$

From channels (III), (IV), (V), (VI), the fifth-order beating signal intensity is

$$\begin{aligned}
 I(\tau, r) \propto & |B_2|^2 \exp[-2(\alpha_1 + \alpha_2)|\tau|] \\
 & + |\eta B_3|^2 \exp(-4\alpha_2|\tau|) + \exp[-(\alpha_1 + 3\alpha_2)|\tau|] \\
 & \times \{ \eta B_2^* B_3 \exp[-i\Delta k \cdot r + i(\omega_2 + \omega_1)\tau] \\
 & + \eta^* B_2 B_3^* \exp[i\Delta k \cdot r - i(\omega_2 + \omega_1)\tau] \}. \quad (2)
 \end{aligned}$$

Here  $B_i$  ( $i = 1, 2, 3$ ) and  $\eta$  are constants independence with  $\tau$ . ASPB signal versus  $\tau$  typically shows the attosecond scale modulation not only with a sum-frequency  $\omega_2 + \omega_1$ , but also spatially with period  $2\pi/\Delta k$  along the direction  $\Delta \mathbf{k} = \mathbf{k}_1 - \mathbf{k}'_1 + \mathbf{k}'_2 - \mathbf{k}_2$ , which is almost perpendicular to the propagation direction of the beat signal. Here  $\Delta k \approx 2\pi|\lambda_1 - \lambda_2|\theta/\lambda_2\lambda_1$ ,  $\theta$  is the angle between beams 1 and 2. Physically, the polarization-beat model assumes that both the pump beams are planar waves. Therefore one-photon SWM signals, which propagate along  $\mathbf{k}_{s_1} = \mathbf{k}_3 + 2\mathbf{k}_1 - 2\mathbf{k}'_1$ , and two-photon SWM signals, which propagate along  $\mathbf{k}_{s_2} = \mathbf{k}_3 + \mathbf{k}_1 - \mathbf{k}'_1 + \mathbf{k}'_2 - \mathbf{k}_2$  or  $\mathbf{k}_{s_3} = \mathbf{k}_3 + 2\mathbf{k}'_2 - 2\mathbf{k}_2$ , are planar waves also. Since one- and two-photon SWM signals (i.e.,  $\mathbf{k}_{s_1}$  and  $\mathbf{k}_{s_2}$  belong to the first beating approach) or two two-photon SWM signals (i.e.,  $\mathbf{k}_{s_2}$  and  $\mathbf{k}_{s_3}$  belong to the second beating approach) propagate along slightly different directions, the interference between them leads to the spatial oscillation.

We then consider the case that beams 1 and 2 are broadband so that  $\alpha_1 \gg \Gamma_{10}$  and  $\alpha_2 \gg \Gamma_{20}$ . Although the beat signal modulation is complicated in general, at the tail of the signal (i.e.,  $\tau \gg \alpha_1^{-1}$  and  $\tau \gg \alpha_2^{-1}$ , which is the case where the correlation time of the incoherent light is much shorter than the time delay of beam 2 with respect to beam 1), the following result can be got.

From channels (I), (II), (III), (V), (VI), the fifth-order beating signal intensity is

$$\begin{aligned}
 I(\tau, r) \propto & |B_1|^2 \exp[-4\Gamma_{10}\tau] \\
 & + |\eta B_2|^2 \exp[-2(\Gamma_{10} + \Gamma_{21})\tau] + \exp[-(3\Gamma_{10} + \Gamma_{21})\tau] \\
 & \times \{ B_1^* \eta B_2 \exp[-i\Delta k \cdot r + i(\Omega_2 + \Omega_1)\tau] \\
 & + B_1 \eta^* B_2^* \exp[i\Delta k \cdot r - i(\Omega_2 + \Omega_1)\tau] \}. \quad (3)
 \end{aligned}$$

From channels (III), (IV), (V), (VI), the fifth-order beating signal intensity is

$$\begin{aligned}
 I(\tau, r) \propto & |B_2|^2 \exp[-2(\Gamma_{10} + \Gamma_{21})\tau] \\
 & + |\eta B_3|^2 \exp[-4\Gamma_{20}\tau] + \exp[-(\Gamma_{10} + \Gamma_{21} + 2\Gamma_{20})\tau] \\
 & \times \{ B_2^* \eta B_3 \exp[-i\Delta k \cdot r + i(\Omega_2 + \Omega_1)\tau] \\
 & + B_2 \eta^* B_3^* \exp[i\Delta k \cdot r - i(\Omega_2 + \Omega_1)\tau] \}. \quad (4)
 \end{aligned}$$

Here  $\Gamma_{10}$ ,  $\Gamma_{20}$ ,  $\Gamma_{21}$  are the transverse relaxations of the atomic energy level system. Equations (3) and (4) indicate that the modulation frequency of the beat signal equals  $\Omega_2 + \Omega_1$ . Therefore the modulation frequency, which corresponds directly to the beating between the resonant frequencies of a cascade three-level system, can be measured with accuracy given by  $\pi(3\Gamma_{10} + \Gamma_{21})$  or  $\pi(\Gamma_{10} + \Gamma_{21} + 2\Gamma_{20})$  approximately. In the other words, the overall accuracy of using FASPB with broadband lights to measure the energy-level difference between two states is limited by the homogeneous line widths.

The FASPB signal is shown to be sensitive to the statistical properties of the Markovian stochastic light fields with arbitrary bandwidth. This is quite different from the fourth-order partial-coherence effects in the

formation of integrated-intensity gratings with pulsed light sources. Their results prove to be insensitive to the specific radiation models. The certain fifth-order coherent anti-Stokes Raman scattering spectroscopy is designed to probe overtone vibration dynamics. The homodyne intensity from the two competing processes is calculated and it is shown how only the direct fifth-order polarization probes overtone dephasing<sup>[8]</sup>. Based on Eq. (4), we have calculated the FASPB in sodium vapor, where the ground state  $3S_{1/2}$ , the intermediate state  $3P_{3/2}$ , and the excited state  $4D_{3/2,5/2}$  form a cascade three-level system.

Figure 3 presents the FASPB signal intensity  $I(\tau, 0)$  versus relative time delay  $\tau$ . It shows that FASPB signal is modulated by the frequency of  $\Omega_2 + \Omega_1$  with a decay factor  $\exp[-(\Gamma_{10} + \Gamma_{21} + 2\Gamma_{20})\tau]$ . Figure 4 indicates that homodyne detects FASPB signal oscillates not only temporally with an ultrafast period  $2\pi/|\Omega_2 + \Omega_1| = 965$  as for sodium atom but also spatially with a period  $2\pi/\Delta k = 0.635$  mm along the direction  $\Delta \mathbf{k}$ , which is almost perpendicular to the propagation direction of the FASPB signal. The three-dimensional (3D) plot (time-spatial interferogram) of the FASPB signal intensity  $I(\tau, r)$  versus time delay  $\tau$  and transverse position  $r$  has larger constant background caused by the intensity fluctuation of the chaotic field. At zero relative time delay ( $\tau = 0$ ), the twin beams originating from the same source enjoy perfect overlap at the sample of their corresponding noise patterns. This gives maximum interferometric contrast. The ultrafast modulation

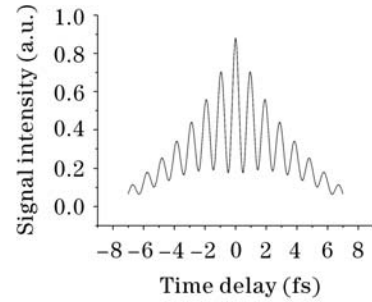


Fig. 3. FASPB signal intensity versus relative time delay. The parameters are taken as  $r = 0$ ,  $\Gamma_{10}^a = 1.56 \times 10^{-2} \text{ fs}^{-1}$ ,  $\Gamma_{30}^a = 1.78 \times 10^{-2} \text{ fs}^{-1}$ ,  $\alpha_1 = 3.2 \text{ fs}^{-1}$ , and  $\alpha_2 = 3.3 \text{ fs}^{-1}$ .

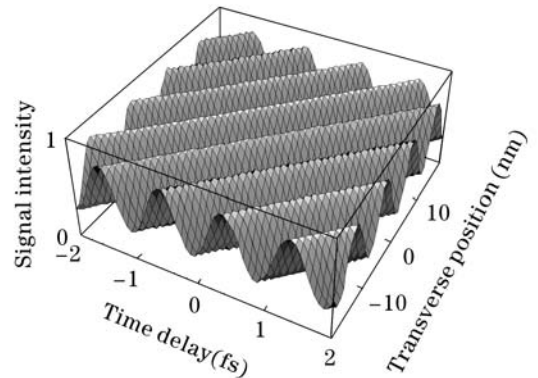


Fig. 4. A three-dimensional plot of the ASPB signal intensity versus time delay and transverse position for the chaotic field. The intensity has been normalized to unit. The parameters are  $\Omega_2 + \Omega_1 = 6.5978 \text{ fs}^{-1}$ ,  $\Delta k = 9.91802 \text{ mm}^{-1}$ ,  $\alpha_1 = 3.2 \text{ fs}^{-1}$ , and  $\alpha_2 = 3.3 \text{ fs}^{-1}$ .

Table 1. Comparison of sequential cascaded FWM signals in FASPB and FFDPB

	FASPB	FFDPB
I	$\rho_{00}^{(0)} \xrightarrow{A_1} \rho_{10}^{(1)} \xrightarrow{(A'_1)^*} \rho_{00}^{(2)} \xrightarrow{A_1} \rho_{10}^{(3)}$ $\mathbf{k}_{CI} = \mathbf{k}_1 - \mathbf{k}'_1 + \mathbf{k}_1$ $\rho_{00}^{(2)} \xrightarrow{A_{CI}} \rho_{10}^{(3)} \xrightarrow{(A'_1)^*} \rho_{00}^{(4)} \xrightarrow{A_3} \rho_{10}^{(5)}$ $\mathbf{k}_{SC} = \mathbf{k}_{CI} - \mathbf{k}'_1 + \mathbf{k}_3$	$\rho_{00}^{(0)} \xrightarrow{A_1} \rho_{10}^{(1)} \xrightarrow{(A'_1)^*} \rho_{00}^{(2)} \xrightarrow{A_1} \rho_{10}^{(3)}$ $\mathbf{k}_{CI} = \mathbf{k}_1 - \mathbf{k}'_1 + \mathbf{k}_1$ $\rho_{00}^{(2)} \xrightarrow{A_{CI}} \rho_{10}^{(3)} \xrightarrow{(A'_1)^*} \rho_{00}^{(4)} \xrightarrow{A_3} \rho_{10}^{(5)}$ $\mathbf{k}_{SC} = \mathbf{k}_{CI} - \mathbf{k}'_1 + \mathbf{k}_3$
II	$\rho_{00}^{(0)} \xrightarrow{A_1} \rho_{10}^{(1)} \xrightarrow{(A'_1)^*} \rho_{11}^{(2)} \xrightarrow{A_1} \rho_{10}^{(3)}$ $\mathbf{k}_{CII} = \mathbf{k}_1 - \mathbf{k}'_1 + \mathbf{k}_1$ $\rho_{11}^{(2)} \xrightarrow{A_{CII}} \rho_{10}^{(3)} \xrightarrow{(A'_1)^*} \rho_{11}^{(4)} \xrightarrow{A_3} \rho_{10}^{(5)}$ $\mathbf{k}_{SC} = \mathbf{k}_{CII} - \mathbf{k}'_1 + \mathbf{k}_3$	$\rho_{00}^{(0)} \xrightarrow{A_1} \rho_{10}^{(1)} \xrightarrow{(A'_1)^*} \rho_{11}^{(2)} \xrightarrow{A_1} \rho_{10}^{(3)}$ $\mathbf{k}_{CII} = \mathbf{k}_1 - \mathbf{k}'_1 + \mathbf{k}_1$ $\rho_{11}^{(2)} \xrightarrow{A_{CII}} \rho_{10}^{(3)} \xrightarrow{(A'_1)^*} \rho_{11}^{(4)} \xrightarrow{A_3} \rho_{10}^{(5)}$ $\mathbf{k}_{SC} = \mathbf{k}_{CII} - \mathbf{k}'_1 + \mathbf{k}_3$
III	$\rho_{00}^{(0)} \xrightarrow{A_3} \rho_{10}^{(1)} \xrightarrow{A'_2} \rho_{20}^{(2)} \xrightarrow{(A_2)^*} \rho_{10}^{(3)}$ $\mathbf{k}_{CIII} = \mathbf{k}'_2 - \mathbf{k}_2 + \mathbf{k}_3$ $\rho_{20}^{(2)} \xrightarrow{A_{CIII}} \rho_{10}^{(3)} \xrightarrow{A'_2} \rho_{20}^{(4)} \xrightarrow{(A_2)^*} \rho_{10}^{(5)}$ $\mathbf{k}_{SC} = \mathbf{k}_{CIII} - \mathbf{k}_2 + \mathbf{k}'_2$	$\rho_{00}^{(0)} \xrightarrow{A_3} \rho_{10}^{(1)} \xrightarrow{A_2} \rho_{20}^{(2)} \xrightarrow{(A'_2)^*} \rho_{10}^{(3)}$ $\mathbf{k}_{CIII} = \mathbf{k}_2 - \mathbf{k}'_2 + \mathbf{k}_3$ $\rho_{20}^{(2)} \xrightarrow{A_{CIII}} \rho_{10}^{(3)} \xrightarrow{A_2} \rho_{20}^{(4)} \xrightarrow{(A'_2)^*} \rho_{10}^{(5)}$ $\mathbf{k}_{SC} = \mathbf{k}_{CIII} - \mathbf{k}'_2 + \mathbf{k}_2$

period of 965 as can still be improved, because the energy-level interval between ground state  $|0\rangle$  and excited state  $|2\rangle$  can be widely separated to increase  $\Omega_2 + \Omega_1$ . Furthermore FASPB can tolerate small perturbations of the optical path due to mechanical vibration and distortion of the optical components as long as these are small compared with  $c/|\omega_2 + \omega_1|$ . The experiment of FASPB is now underway in our group.

Although not as 'clean' as coherent femtosecond pulse experiment from a theoretical perspective, it is anticipated that with a more physical picture provided by the subtle fourth-order ensemble average  $\langle |P^{(5)}|^2 \rangle$  of FASPB (especially the effects of the different Markovian noise models) and the inherent experimental advantages of color-locked noisy light, such as robustness of signal, insensitivity to dispersion induced by the optical elements and being less costly to set up and maintain, FASPB will continue to be apparently designed to probe overtone dephasing dynamics, and provide useful insight into the coherent control dynamics of gas phase sample.

Using fifth-order density-matrix perturbation method for a cascade three-level system, we can obtain for the fifth-order nonlinear polarizations in the rotating-waves, slowly-varying envelope, and dipole approximation, respectively. Under certain conditions a SWM signal consists of two sequential cascaded FWM signals. The density matrix elements can be calculated by following the perturbation channels (Liouville pathways) (see Table 1).

Taking path (III) for instance, the phase matching conditions are  $\mathbf{k}_{CIII} = \mathbf{k}'_2 - \mathbf{k}_2 + \mathbf{k}_3$  and  $\mathbf{k}_{SC} = \mathbf{k}'_2 - \mathbf{k}_2 + \mathbf{k}_{CIII}$ . Two-photon non-degenerate SWM signals (beam 5) with frequency  $\omega_3$  will be emitted along the direction  $2\mathbf{k}'_2 - 2\mathbf{k}_2 + \mathbf{k}_3$ , and the cascaded FWM signals will be emitted along the directions  $\mathbf{k}_{CIII} = \mathbf{k}'_2 - \mathbf{k}_2 + \mathbf{k}_3$  and  $\mathbf{k}_{SC} = \mathbf{k}'_2 - \mathbf{k}_2 + \mathbf{k}_{CIII}$ . For the limit of the paper length, only the phase matching conditions of path I, II, and III are listed in Table 1. It also shows the comparison of FASPB and fifth-order femtosecond difference-frequency polarization beats (FFDPB).

The direct fifth-order polarization beat processes can often be obscured by cascaded or sequential lower order processes that compete with the direct event and give similar time domain behavior though they probe different

dynamics<sup>[8,9]</sup>. The one-order diffraction signal (beam 4) is contributed primarily by the third-order nonlinear polarization whereas the second-order diffraction signal (beam 5) may include contributions from the direct fifth-order nonlinear polarization and cascaded processes due to the third-order nonlinear polarization. In some cases the cascaded lower order effects may completely obscure the more interesting fifth-order signal.

In conclusion, we have studied theoretically a phase-conjugate ultrafast modulation spectroscopy due to the interference between fifth- and fifth-order optical polarizations in cascade three-level system. FASPB signal is modulated by the frequency of  $\Omega_2 + \Omega_1$  with a decay factor  $\exp[-(\Gamma_{10} + \Gamma_{21} + 2\Gamma_{20})\tau]$ . It is found that the temporal behavior of the sum-frequency polarization beat signal depends on the stochastic properties of lasers and transverse relaxation rate of the atomic energy-level system. The beat signal depends on the fourth-order coherence function determined by the laser line shape.

This work was supported by the National Natural Science Foundation of China (No. 60308002) and the Foundation of National Excellent Doctoral Dissertation of China (No. 200339). J. Song's e-mail address is jpsong@mail.xjtu.edu.cn.

## References

1. D. DeBeer, L. G. Van Wagenen, R. Beach, and S. R. Hartmann, Phys. Rev. Lett. **56**, 1128 (1986).
2. Y. Zhang, T. Tang, L. Sun, and P. Fu, Phys. Rev. A **61**, 023809 (2000).
3. Y. Zhang, C. Gan, S. M. Farooqi, K. Lu, X. Hou, and T. Tang, J. Opt. Soc. Am. B **19**, 1204 (2002).
4. K. Lu, X. Zhu, W. Zhao, Y. Yang, J. Li, Y. Zhang, and J. Zhang, Chin. Opt. Lett. **483** (2004).
5. Y. Zhang, K. Lu, T. Tang, and P. Fu, Acta. Opt. Sin. **20**, 335 (2000).
6. Y. Zhang, C. B. de Araujo, and E. E. Eyler, Phys. Rev. A **63**, 043802 (2001).
7. Y. Zhang, C. Gan, K. Lu, C. Li, and X. Hou, Opt. Commun. **205**, 163 (2002).
8. D. J. Ulness, J. C. Kirkwood, and A. C. Albrecht, J. Chem. Phys. **108**, 3897 (1998).
9. C. Chen, Y.-Y. Yin, and D. S. Elliott, Phys. Rev. Lett. **64**, 507 (1990).